Dissecting Clonal Hematopoiesis in Tissues of Patients with Classic Hodgkin Lymphoma

Alessandra Venanzi, Andrea Marra, Gianluca Schiavoni, Sara G. Milner, Roberto Limongello, Alessia Santi, Valentina Pettirossi, Simona Ultimo, Luisa Tasselli, Alessandra Pucciarini, Lorenza Falini, Sofia Sciabolacci, Maria Paola Martelli, Paolo Sportoletti, Stefano Ascani, Brunangelo Falini, and Enrico Tiacci

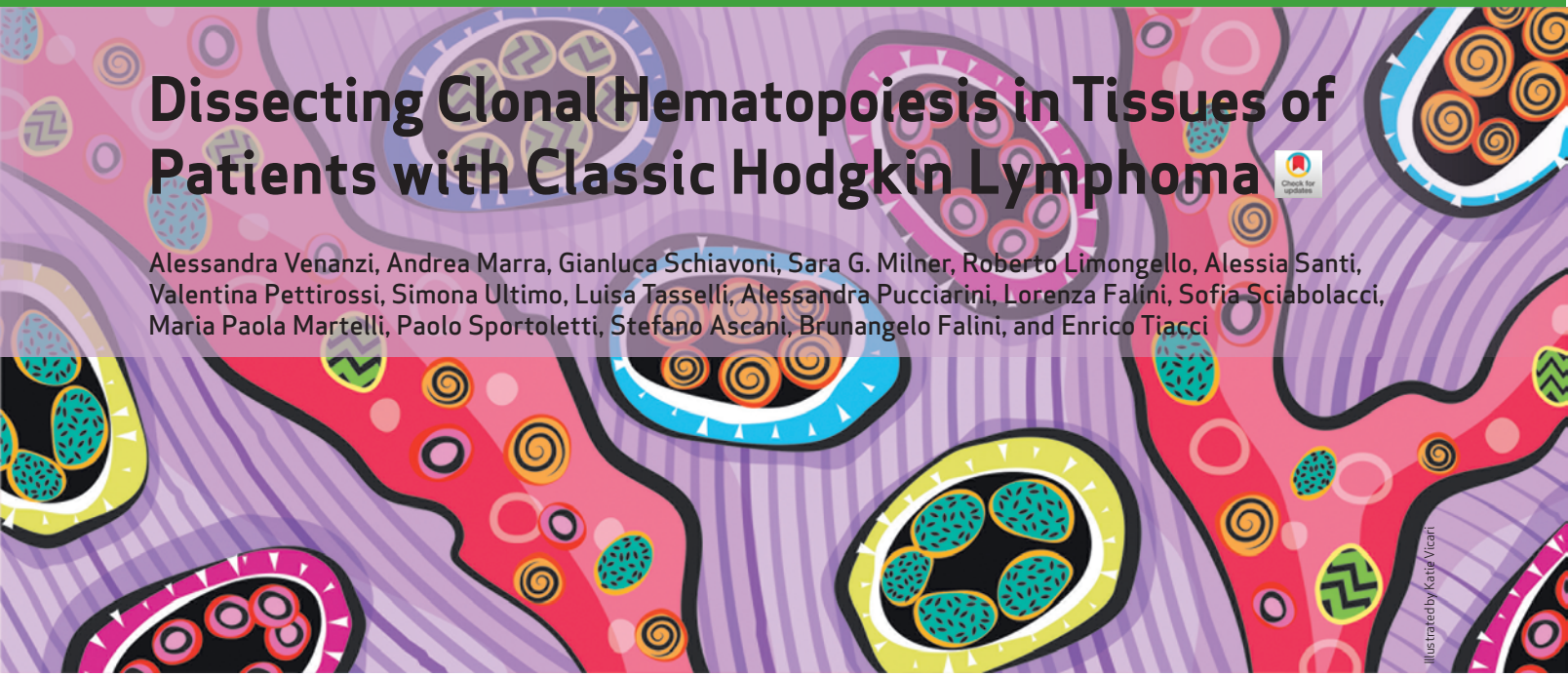

ABSTRACT Clonal hematopoiesis predisposes to hematologic malignancies. However, clonal hematopoiesis is understudied in classic Hodgkin lymphoma (cHL), a mature B-cell neoplasm exhibiting the most abundant microenvironment. We analyzed clonal hematopoiesis in 40 cHL cases by sequencing microdissected tumor cells and matched normal cells from blood and/or lymph nodes. Five patients had blood and/or tissue clonal hematopoiesis. In three of five patients (all failing first-line therapy), clonal hematopoiesis spread through the tissue microenvironment extensively, and featured mutant *DNMT3A*^{R882H}, *KRAS*^{G60D}, and *DNMT3A*^{R882H}+*TET2*^{Q1274*} in 33%, 92%, and 60% of non-neoplastic cells, respectively. In the latter case, *DNMT3A/TET2*-mutant clonal hematopoiesis seeded the neoplastic clone, which was infected by the Epstein–Barr virus and showed almost no other somatic mutations exome-wide. In the former case, *DNMT3A*-mutant clonal hematopoiesis did not originate the neoplastic clone despite dominating the blood and B-cell lineage (~94% leukocytes; ~96% mature blood B cells), yet led to *NPM1*-mutated acute myeloid leukemia 6 years after therapy for cHL. Our results expand to cHL the spectrum of hematologic malignancies associated with clonal hematopoiesis.

SIGNIFICANCE: Clonal hematopoiesis can be present in the cHL tissue, can give rise to the tumor clone, and can spread to large parts of its microenvironment. Even when massive, clonal hematopoiesis does not always give rise to the neoplastic clone of multiple myeloid and lymphoid neoplasms occurring in the same patient.

INTRODUCTION

Clonal hematopoiesis of indeterminate potential (CHIP) is promoted by the age-dependent stochastic occurrence of mutations in driver genes (e.g., *DNMT3A* and *TET2*) that confer a fitness advantage to hematopoietic stem/progenitor cells (HSPC; ref. 1). CHIP is frequent in the elderly and predisposes to hematopoietic neoplasms mostly of myeloid or T-cell

Institute of Hematology and Center for Hemato-Oncology Research, University and Hospital of Perugia, Perugia, Italy.

Note: Supplementary data for this article are available at Blood Cancer Discovery Online (https://bloodcancerdiscov.aacrjournals.org/).

A. Venanzi, A. Marra, and G. Schiavoni contributed equally to this article.

B. Falini and E. Tiacci are cosenior authors of this article.

Corresponding Authors: Enrico Tiacci, Institute of Hematology and Center for Hemato-Oncology Research (C.R.E.O.), University and Hospital of Perugia, Perugia, 06132, Italy. Phone: 3907-5578-3294; Fax: 3907-5578-3834; E-mail: enrico.tiacci@unipg.it; and Brunangelo Falini, brunangelo.falini@unipg.it

Blood Cancer Discov 2021;2:216–25

doi: 10.1158/2643-3230.BCD-20-0203

origin, the risk of which depends on the number and type of mutated gene(s) and on clone size (1–9). Tumor development requires the subsequent acquisition of additional disease-specifying genetic lesions. Sometimes multiple myeloid and/or lymphoid neoplasms arise from CHIP in the same patient (10), occasionally even at a young age as we described in a case of angioimmunoblastic T-cell lymphoma with massive clonal hematopoiesis (variant allele frequency/VAF >45%) who subsequently developed *NPM1*-mutated acute myeloid leukemia (AML; ref. 11).

Classical Hodgkin lymphoma (cHL) is a unique tumor entity featuring a small neoplastic clone of Hodgkin/Reed–Sternberg (HRS) cells dispersed in an exuberant supportive microenvironment largely of hematopoietic origin, with T cells representing a major component especially in the two most common histologic subtypes of this cancer (nodular sclerosis and mixed cellularity; refs. 12, 13). Recent genetic analyses of cHL focused on mutations somatically present in HRS cells but not in matched normal cells, uncovering several new mutated genes driving lymphoma cell growth and immune evasion (14–17). Clonal hematopoiesis has been detected in HSPCs harvested from 9 of 64 (14%) cHL relapsed patients of unknown age undergoing autologous transplantation (18). However, no data exist on the potential presence of clonal hematopoiesis in the microenvironmental and/or neoplastic components of cHL tissue. Here, we assessed clonal hematopoiesis frequency and tissue distribution in 40 well-characterized cHL cases largely studied at disease onset, and also describe the surprising findings on a young cHL patient with massive CHIP who developed AML following therapy for cHL.

RESULTS

Prevalence of Clonal Hematopoiesis in Patients with cHL

To assess the frequency of clonal hematopoiesis in patients with cHL, we interrogated our previous whole-exome sequencing (WES) data from non-HRS cells of 34 cHL cases, which we used as a matched normal counterpart to call somatic mutations in HRS cells (15). In particular, we reanalyzed WES data from whole-blood leukocytes (in 26/34 cases; mean unique coverage depth: 157×) or, if no blood sample was available, from reactive cells mostly of lymphoid morphology microdissected from frozen tissue biopsies (in 8/34 cases; mean unique coverage depth: 149×), focusing on a target region of interest represented by 35 genes implicated in CHIP (as defined by Tuval and Shlush; ref. 9 and Table 1 therein). When mutations of such genes were detected in the blood at or above the canonical VAF cutoff of 2% (2), their presence was assessed in nonneoplastic cells microdissected from the tissue biopsy of the same patient; finally, mutations with ≥2% VAF in the blood and/or in microdissected nonneoplastic cells were searched for in matched microdissected HRS cells of the same case (mean unique coverage depth: 125×). We also newly microdissected HRS and reactive cells mostly of lymphoid morphology (Supplementary Fig. S1) from frozen biopsies of six additional cHL patients (using the same previous experimental pipeline; ref. 15), followed by targeted sequencing of 43 genes recurrently mutated in myeloid neoplasms and/or implicated in CHIP (Supplementary Table S1A; mean unique coverage depth: 3,425×).

Among the 40 patients with cHL studied in total, tissue biopsies were analyzed at onset of lymphoma in 32 cases, at relapse in 7 cases and at both time points in 1 case; for each patient with an available whole-blood sample, the latter was analyzed at the same time point as the tissue biopsy, except in the case studied both at onset and at relapse whereby blood was available only at relapse.

Median age was 35 years (range 15–83); 13 patients were >55 and 5 patients >70 years old. Clonal hematopoiesis was detected in the peripheral blood and/or cHL tissue in 5 of 40 cases (12.5%; Table 1). We note that the coverage depth of WES, which was used in the vast majority of our cases, can miss small-sized clonal hematopoiesis, and, therefore, a higher prevalence of clonal hematopoiesis might result upon deeper targeted sequencing. Clonal hematopoiesis was frequent in patients above 70 years (3/5, 60%; cases 3, 4, and 5), whereas only 2 of 35 (5.7%) patients younger than 70 years (cases 1–2) showed clonal hematopoiesis ($P = 0.009$ by Fisher exact test; Table 1), in line with the known increase of CHIP frequency with age (1–9).

Tissue Distribution of Clonal Hematopoiesis in Patients with cHL

We then dissected the distribution of clonal hematopoiesis through the cHL tissue in each of these five cases. Case 1 was notable for the development of cHL followed by AML and will be described separately in the next section.

Case 2 was a 31-year-old male, who presented with stage IVB at onset and was studied at progression following both doxorubicin hydrochloride, bleomycin, vinblastine sulfate, and dacarbazine (ABVD) and salvage autologous hematopoietic stem cell transplantation (ASCT). He had a mixed cellularity cHL negative for Epstein–Barr virus (EBV) infection, in which a *KRAS*^{G60D} mutation massively expanded throughout reactive tissue cells (VAF = 45.9%) while being absent in HRS cells; conversely, the latter carried 57 somatic protein-changing mutations upon WES (ref. 15; Fig. 1A; Supplementary Table S2).

Case 3 was an 83-year-old male, who had an EBV-positive mixed cellularity cHL, stage IIB, and died of chemotherapy complications. Targeted sequencing of the onset tissue biopsy documented a likely pathogenic mutation of *CBL* (G375S; ref. 19) that was present at a relatively low VAF (2.5%) in reactive tissue cells and was absent in HRS cells (Supplementary Fig. S2; Supplementary Table S2).

Case 4 was an 81-year-old female. She had an EBV-negative nodular sclerosis cHL, stage IIA, and remained free from progression 64 months after doxorubicin hydrochloride, vinblastine sulfate, and dacarbazine (AVD) polychemotherapy. She carried a *TET2*^{N1487Ifs84} mutation in blood leukocytes (VAF = 3.2%) but not in reactive tissue cells or in HRS cells; the latter had 97 somatic mutations on WES (ref. 15; Fig. 1B; Supplementary Table S2).

Case 5 was a 73-year-old male, who presented with mixed cellularity cHL stage IIA and was studied at relapse 35 months after six cycles of ABVD. In his tissue biopsy, *DNMT3A*^{R882H} and *TET2*^{Q1274*} spread considerably in reactive tissue cells (VAF = 30% and 8.4%, respectively); however, unlike the previous cases (including case 1 also showing *DNMT3A*^{R882H}-mutant clonal hematopoiesis; see next section), both mutations

Table 1. Prevalence and tissue distribution of clonal hematopoiesis in patients ($n = 40$) with cHL

CH present	Years of age	Pt.#	Time of sampling	Progressed after first-line chemotherapy	Gene mutation	VAF in whole blood	VAF in microdissected		VAF in whole tissue section	AML onset	AML remission	
							Reactive lymphoid cells	HRS cells		VAF in bone marrow	VAF in blood T cells	VAF in blood B cells
NO ($n = 35$)	Median 35 Range 15–75											
YES ($n = 5$)	30	Case 2	2nd relapse	YES	*KRAS* G60D	NA	45.9%	ND	22.9%			
	83	Case 3	Onset	Not evaluable	*CBL* G375S	NA	2.5%	ND	NA			
	81	Case 4	Onset	NO	*TET2* N1487Ifs84	3.2%	ND	ND	NA			
	73	Case 5	Onset	YES	*DNMT3A* R882H	NA	NA	NA	32.4%			
					TET2 Q1274[a]				22.3%			
			1st relapse		*DNMT3A* R882H	NA	30%	43%	37.9%			
					TET2 Q1274[a]		8.4%	31.1%	26.9%			
	45	Case 1	Onset	YES	*DNMT3A* R882H	47%	16.4%	ND	12.2%	45.2%	6.9%	48%
					NPM1 W288CfsTer12	ND				40.6%	ND	
					PTPN11 E76K	ND				25.7%	ND	
					FLT3 ITD	NA				0.14[a]	NA	
					FLT3 ITD	NA				0.11[a]	NA	
					STAT6 N417Y	NA	ND	36.9%	NA	NA		
					STAT6 D419H			35.7%				
					SOCS1 P83Afs*25			98.6%				

Abbreviations: CH, clonal hematopoiesis; NA, not available; ND, not detected.
[a]Mutant/wild-type ratio by fragment length analysis.

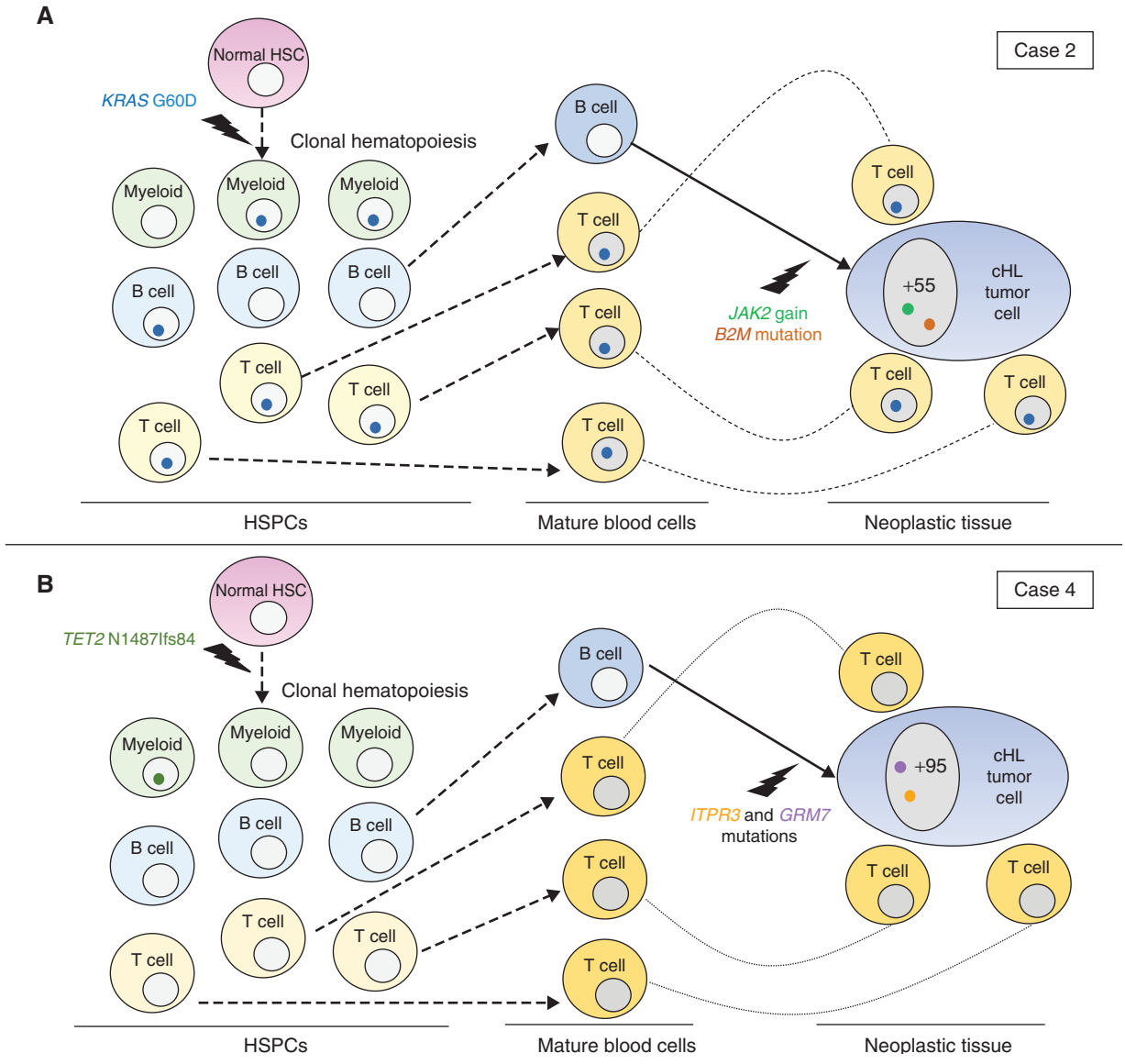

Figure 1. Tissue involvement by clonal hematopoiesis in cHL. **A,** In this EBV-negative mixed cellularity cHL (case 2), the reactive tissue microenvironment (mostly represented by T cells—not shown) belonged to clonal hematopoiesis almost entirely, as it featured a *KRAS*^{G60D} mutation at a VAF of 45.9%. However, the HRS cell clone developed from a B cell not belonging to clonal hematopoiesis, after acquiring a *JAK2* gain and a *B2M* mutation (genetic lesions typical of cHL), along with 55 additional somatic protein-changing mutations detected by WES in the HRS cell clone (ref. 15; "+55" in the HRS cell nucleus). Myeloid involvement by clonal hematopoiesis is presumptive because we did not have a blood or bone marrow sample from this patient to formally confirm it. HSC, hematopoietic stem cell. **B,** In EBV-negative nodular-sclerosis case 4, clonal hematopoiesis (carrying *TET2*^{N1487Ifs84}), which was detected in whole-blood leukocytes and likely involved the myeloid lineage (only or mainly), did not spread through either the lymphoid HRS cell clone or its reactive tissue microenvironment. Also indicated are mutations of two genes (*ITPR3* and *GRM7*, recurrently targeted in cHL; ref. 15) that were found in HRS cells but not in blood leukocytes of this cHL case, along with an additional 95 somatic protein-changing mutations detected by WES in the HRS cell clone (ref. 15; "+95" in the HRS cell nucleus). (*continued on next page*)

were carried over in the HRS cell clone, which was infected by EBV and otherwise had only three somatic mutations detected by WES (ref. 15; Fig. 1C; Supplementary Table S2). Retrospective targeted sequencing of whole sections from the formalin-fixed lymph node biopsy at cHL onset of case 5 documented the same *DNMT3A*^{R882H} and *TET2*^{Q1274*} mutations at 32% and 22% VAF, respectively (Table 1 and Supplementary Table S2), indicating a consistent association of microenvironmental clonal hematopoiesis with cHL pathogenesis in this patient and confirming the inability of chemotherapy to clear clonal hematopoiesis (9).

Trajectories of Clonal Hematopoiesis in a cHL Patient Sequentially Developing AML

Case 1 was a 45-year-old man diagnosed with nodular sclerosis, stage IVB cHL, negative for EBV (Fig. 2A–C). After failing polychemotherapy with ABVD, he was successfully salvaged with a second-line regimen (ifosfamide, gemcitabine,

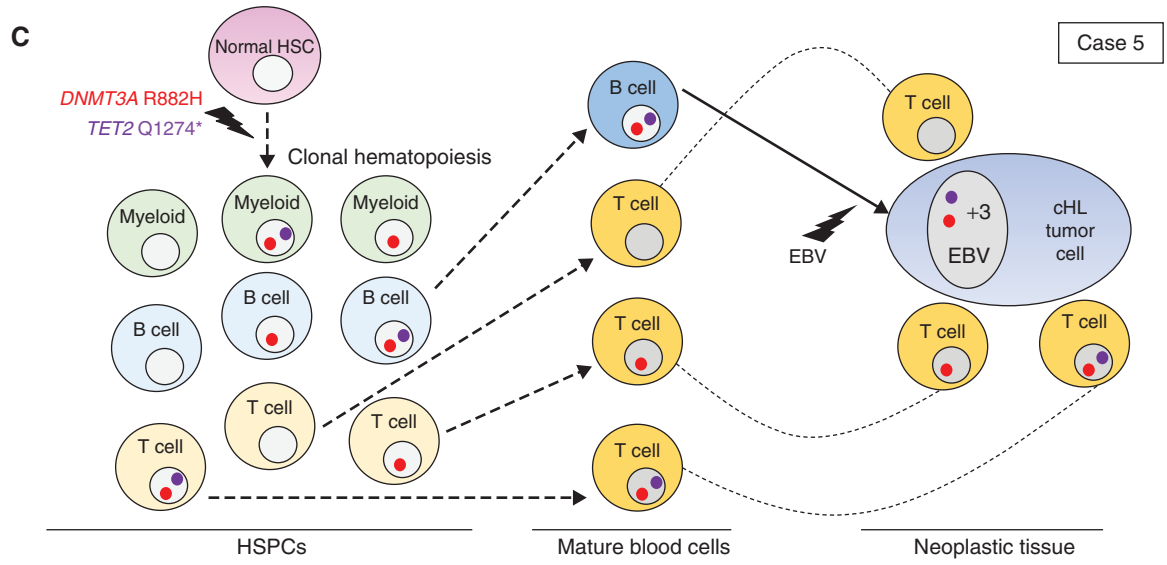

Figure 1. ***(Continued)*** **C,** Tissue distribution of clonal hematopoiesis in case 5, showing a double-mutant *DNMT3A*^{R882H} and *TET2*^{Q1274*} clone with likely multilineage involvement of B, T, and myeloid cells, which spread through both the microenvironmental and HRS cell components of cHL. The latter component was infected by EBV and lacked almost any other somatic mutations that could have caused the neoplastic transformation of its mature B cell of origin (only three protein-changing mutations being present exome-wide in the HRS cell clone but not in reactive tissue cells, indicated as "+3" within the HRS cell nucleus, and none of them targeted a gene recurrently mutated in cHL; ref. 15). Involvement of myeloid cells by clonal hematopoiesis is presumptive because we did not have a blood or bone marrow sample from this patient to formally confirm it.

vinorelbine; IGEV) and ASCT, followed by consolidating radiotherapy. Almost 6 years after cHL diagnosis, he developed AML with clonal mutations of *NPM1* and *DNMT3A*^{R882H}, and subclonal *PTPN11* and *FLT3*-ITD mutations. The bone marrow karyotype was normal and no mutations of *TP53* or *PPM1D* were identified, in contrast to what is typically observed in therapy-related AML (5). Despite multiple treatments, the patient died 7 months later of progressive AML (Supplementary Data). Retrospective analysis of blood DNA at cHL diagnosis revealed *DNMT3A*^{R882H} at high VAF (47%, i.e., ~94% of blood cells), indicating massive clonal hematopoiesis from which AML later arose after acquiring the *NPM1* mutation (Fig. 2D; Table 1; Supplementary Table S2), which is typically associated with *de novo* AML (20).

To deconstruct *DNMT3A*^{R882H} distribution through lymphopoiesis, we sequenced purified mature B and T cells from a fresh peripheral blood sample taken during remission from AML. *DNMT3A*^{R882H} was observed in almost all B cells (VAF = 48%) and some T cells (VAF = 6.9%; Table 1; Supplementary Table S2). Targeted sequencing of the cHL neoplastic and nonneoplastic components microdissected from a lymph node biopsy (Supplementary Fig. S1) documented *DNMT3A*^{R882H} in a considerable proportion (VAF = 16.4%) of reactive cells mostly of T-cell origin (Fig. 2C; Supplementary Fig. S1) but, surprisingly, its absence in HRS cells (Fig. 2D; Table 1; Supplementary Table S2). The latter cells carried clonal *STAT6* and *SOCS1* mutations typical of cHL (15).

In general, clonal hematopoiesis appeared more frequently in cases studied in the lymph node (4/15, 27%) versus the blood (2/27, 7%; cases 1 and 4 were studied in both compartments). However, this difference was not significant (Fisher exact test $P = 0.16$) and could have been confounded by the significantly older age of the former versus the latter group (mean of 56 and 37 years, respectively; unpaired t test $P = 0.003$).

In all three cases (1, 2, and 5) with significant clonal hematopoiesis spreading (VAF ≥10%) through the mostly lymphoid microenvironment, the latter was found to be polyclonal upon T-cell receptor gamma gene rearrangement analysis (Supplementary Fig. S3), confirming that the mutations underlying clonal hematopoiesis had occurred in a bone marrow stem or progenitor cell before T-cell lineage commitment. All three patients progressed after first-line chemotherapy, as opposed to 11/35 (31%; Fisher exact test P value 0.043) evaluable patients with absent or nonextensive clonal hematopoiesis in the tumor tissue, who had similar clinical characteristics and received a no less intense first-line therapy (Table 2).

DISCUSSION

Here, we provided an initial characterization, largely by WES, of clonal hematopoiesis prevalence and histogenetic distribution in cHL cases mostly studied at disease onset. Clonal hematopoiesis was readily observed in elderly patients with cHL but could be detected also in younger ones, and an even higher prevalence might emerge upon deeper targeted sequencing. CHIP-associated mutations displayed a diverse distribution pattern through the HRS cell and microenvironmental tissue components, with significant representation in both (case 5, Fig. 1C), in only the microenvironment (case 2, Fig. 1A; case 1, Fig. 2D), or in none of them (case 4, Fig. 1B; and also case 3 with little spreading in reactive tissue cells, Supplementary Fig. S2). Notably, in the three patients with significant tissue involvement by clonal hematopoiesis, who all failed first-line chemotherapy, a large part of the

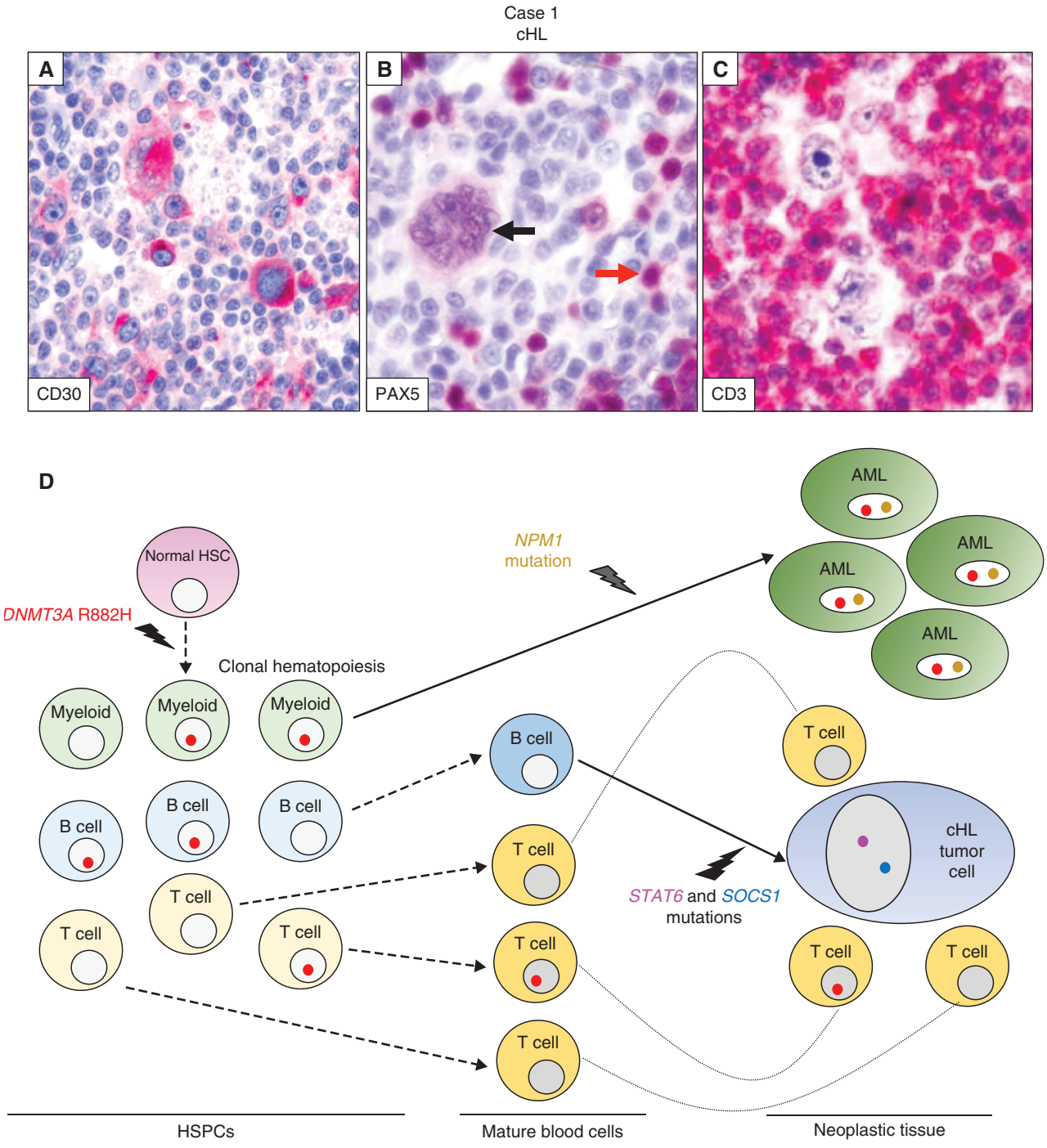

Figure 2. Trajectories of clonal hematopoiesis in a patient sequentially developing cHL and AML (case 1). **A–C,** Nodular sclerosis cHL lymph node biopsy immunostained (red labeling) for CD30 shows various HRS cells strongly expressing this cHL diagnostic marker (**A**). Immunostaining for the B cell–specific transcription factor PAX5 (**B**) shows nuclear positivity in a multinucleated Reed–Sternberg cell (black arrow) and, to a higher intensity, in sparse bystander B cells (one indicated by the red arrow). In **C,** CD3 immunostaining highlights the abundant reactive T cells in the microenvironment surrounding HRS cells. **D,** Spreading of the *DNMT3A*^{R882H} mutation: (i) through preneoplastic hematopoiesis in the bone marrow and blood, with multilineage myeloid cell, B-cell, and T-cell involvement and then (ii) through the neoplastic tissues of AML and cHL, in the latter involving reactive tissue cells (mostly T cells) but not HRS cells. Also indicated are the genetic lesions leading to the development of the AML clone (*NPM1* mutation) and the HRS cell clone (*STAT6* and *SOCS1* mutations), arising, respectively, from a myeloid progenitor belonging to clonal hematopoiesis and a mature B cell not belonging to clonal hematopoiesis. HSC, hematopoietic stem cell.

Table 2. Clinicopathologic features of cHL cases stratified by clonal hematopoiesis distribution in the tissue

		Clonal hematopoiesis in cHL tissue		
N = 40 patients		Extensive[a] (*n* = 3)	Absent/nonextensive (*n* = 37)	*P*[b]
Age	>60 years	1 (33%)	9 (24%)	1
	<60 years	2 (67%)	28 (76%)	
EBV status	EBV+	1 (33%)	8 (22%)	0.55
	EBV−	2 (67%)	29 (78%)	
Histotype	Nodular sclerosis	1 (33%)	21 (57%)	0.58[c]
	Mixed cellularity	2 (67%)	12 (32%)	
	Other	0 (0%)	4 (11%)	
Clinical stage	Early (≤ IIA)	1 (33%)	13 (37%)[d]	1
	Advanced (≥ IIB)	2 (67%)	22 (63%)[d]	
Outcome of first-line therapy[e]	No progression	0 (0%)	24 (69%)[f]	0.043
	Progression	3 (100%)	11 (31%)[f]	
	Follow-up in months[g]	0–6–35	64 (median)[g]	0.034
			0–149 (range)[g]	

[a]Extensive: VAF ≥10%.

[b]By Fisher exact test except for comparison of follow-up where *t* test was used.

[c]Nodular sclerosis versus all other subtypes.

[d]Clinical stage at diagnosis was not available for two patients (UPN26 and UPN40).

[e]ABVD in all cases, with the following exceptions of little relevance: (i) COPP/ABV in pediatric patient UPN27, not showing clonal hematopoiesis and not progressing after first-line therapy; (ii) COPP without vincristine in elderly patient UPN41/case 3, whose outcome was not evaluable; and (iii) omission of bleomycin in 3/35 patients (UPN13, UPN25/case 4, and UPN30, all without extensive clonal hematopoiesis in the cHL tissue and all not progressing after first-line therapy). COPP/ABV stands for cyclophosphamide, vincristine sulfate, prednisone, procarbazine hydrochloride/doxorubicin hydrochloride, bleomycin, vinblastine sulfate.

[f]Outcome was not available for one patient (UPN40) and not evaluable in another patient (UPN41/case 3) who died early due to acute chemotherapy toxicity.

[g]Follow-up was not available for one patient (UPN40) and not evaluable in another (UPN41/case 3).

reactive microenvironment (mostly lymphoid and confirmed to be polyclonal upon T-cell receptor gene rearrangement analysis) belonged to HSPC-derived clonal hematopoiesis (33%–92% of cells based on VAF). Considering that both the HRS cell clone and the microenvironment supporting its growth (13) are central features of cHL pathogenesis, and that chemotherapy does not clear clonal hematopoiesis (9), clonal hematopoiesis spreading in the cHL tissue components might contribute to the development of this lymphoma and influence its prognosis. However, this hypothesis should be ascertained in larger patient cohorts.

Another interesting finding reported here (case 5) is the first description of mutations in the epigenetic DNA modifiers *DNMT3A* and *TET2* in tumor cells of cHL (see also Supplementary Discussion). While relatively frequent in T-cell lymphomas, mutations of *TET2* are less prevalent in the tumor cell clone of B-cell lymphomas (10), and those of *DNMT3A* are even rarer (21, 22). Furthermore, in diffuse large B-cell lymphomas (DLBCL), presumably clonal *DNMT3A* mutations were found exclusively in EBV+ cases together with mutations of *TET2* (a known tumor suppressor in DLBCL pathogenesis; ref. 23) and in the absence of histone-modifying gene mutations (24). This configuration is similar to cHL case 5, which (in addition to an extensive clonal hematopoiesis of the tumor microenvironment) featured an EBV+ lymphoma cell clone carrying *DNMT3A* and *TET2* comutations but an otherwise almost null exome-wide somatic mutation burden (known to be low in EBV+ cHL; ref. 15). However, additional investigations are required to determine whether *DNMT3A* and *TET2* comutations may play a tumor-cell intrinsic role in the pathogenesis of some EBV+ Hodgkin (and non-Hodgkin) B-cell lymphomas.

Regarding the *TET2* disruptive variant observed in the lymphoid microenvironment of case 5, we note that, although Buscarlet and colleagues showed an exclusion of *TET2*-inactivating mutations from the mature T-cell compartment in healthy individuals with CHIP (25), in case 5 the *TET2* variant was presumably subclonal to (i.e., occurred later than) the *DNMT3A* mutation concomitantly present in the microenvironment (because the VAFs of these two mutations in whole lymph node sections were, respectively, 22% and 32% in the onset sample, and 38% and 27% in the relapse sample). This latter finding is in keeping with the multipotent involvement (T-cell lineage included) typical of mutant *DNMT3A* that was also shown by Buscarlet and colleagues (25) and may point to mutant *DNMT3A* being permissive to propagation of a subsequent *TET2* disruptive variant through the T-cell lineage. However, we also note that, in the microdissected tumor microenvironment of case 5, *TET2* mutation VAF was not particularly high (8.4%), and hence we cannot formally exclude that it was entirely contributed by non-T cells.

We also show that the tumor clones of multiple lymphoid and myeloid neoplasms developing in the same patient with

clonal hematopoiesis do not necessarily derive all from clonal hematopoiesis, even when (as in case 1 here) the specific mutations driving clonal hematopoiesis in that patient can be present in the tumor clone of the cancer histologies in question and even when such mutations extensively spread through the cell-of-origin lineages and the microenvironment of the neoplasms affecting that patient. Thus, clonal hematopoiesis trajectories must be carefully disentangled to correctly interpret the histogenesis and pathogenesis of multiple blood cancers arising in patients with clonal hematopoiesis.

Finally, the observations made on case 1 raise the question as to whether his AML was related or not to the previous therapy for cHL (see also Supplementary Discussion). The AML clone lacked the genetic signature of typical therapy-related cases (i.e., *TP53* or *PPM1D* mutations; complex karyotype and/or loss of chromosomes 5 or 7; refs. 1, 5, 8, 26) and instead carried an *NPM1* mutation with normal karyotype, typical of *de novo* AML (20). These findings may suggest a derivation of the leukemia from a large, and thus high-risk, preexisting CHIP clone (driven by mutant *DNMT3A*), similar to another recently described lymphoma patient with massive CHIP (sustained by mutant *TET2* and *ASXL1*) who then developed *NPM1*-mutated AML (11). Further studies are needed to clarify the pathogenesis of such atypical posttherapy AML cases arising from CHIP in patients with lymphoma.

In conclusion, our data demonstrated that clonal hematopoiesis can spread through the neoplastic and/or nonneoplastic tissue components of cHL, with potential implications for the biology and clinical course of this mature B-cell malignancy.

METHODS

Patients' Samples

We analyzed various types of biological samples that were taken from case 1, as well as lymph node biopsies that were taken from five additional newly processed cHL cases, after the signature of a written informed consent form approved by our hospital review board and in accordance with the Declaration of Helsinki. Lymph node and bone marrow biopsies were fixed in formalin and B5, respectively, and routinely processed according to standard immunohistologic procedures; a portion of the lymph node biopsy was in parallel frozen for laser microdissection (see next paragraph). B cells and T cells of case 1 were purified (to a level ≥98%) from peripheral blood by MACS technology using anti-CD19 and anti-CD3 microbeads (Miltenyi Biotec), respectively, and MS columns following manufacturer recommendations. Genomic DNA was extracted from bone marrow aspirate and peripheral blood samples of case 1 using QIAamp DNA Blood MIDI Kit (QIAGEN), and from his purified B and T cells using AllPrep DNA/RNA Mini Kit (QIAGEN). The Gentra Puregene kit (QIAGEN) was instead used to extract DNA from whole biopsy sections of case 5 (formalin-fixed paraffin-embedded at onset; frozen at relapse), case 1 (frozen at onset) and case 2 (frozen at relapse) in order to validate their WES data obtained from microdissected nonneoplastic cells (see the below section "WES Analysis of Clonal Hematopoiesis in a Previous cHL Patient Cohort"). T-cell gene rearrangement studies were performed on DNA from frozen whole lymph node sections with standard PCR, followed by fragment length analysis using the T-cell receptor gamma rearrangements Molecular Analysis Kits (Vitro Master Diagnostica).

Laser Microdissection

Laser microdissection of HRS and reactive cells from lymph node biopsy sections of the six newly processed cases was performed as described previously (15). Briefly, HRS cells were microdissected from frozen sections stained with hematoxylin and eosin using an Olympus microscope equipped with PALM Microlaser Technology. Eight-micron–thick sections were mounted on membrane-covered slides (Membrane Slide 1.0 PEN, Zeiss) and air-dried at room temperature overnight. Sections were then fixed for 10 minutes in acetone, air-dried at room temperature for 5 minutes, incubated with hematoxylin (Dako-Agilent) for 2 minutes, washed in molecular biology–grade water for 2 minutes, incubated with 2% eosin for 1 minute, washed again, and air-dried overnight at room temperature. A total of approximately 1,450 HRS cells were microdissected as single cells (or, less frequently, as small aggregates of 2–4 cells attached to one another) according to their characteristic cytomorphology and large cell size, and then catapulted into an opaque adhesive cap of a 0.5 mL tube (Zeiss) in groups of 200 to 300 cells per cap. A similar number of non-HRS cells mostly of lymphoid morphology and T-cell immunophenotype (representative example in Fig. 2C; Supplementary Fig. S1) were microdissected from the same sections in areas of 200 to 300 cells and collected in separate caps (some contamination by macrophages, eosinophils, and/or other cell types cannot be excluded, but it would likely have limited relevance, especially in cases showing extensive clonal hematopoiesis with VAF ≥10%). Following DNA extraction using the Gentra Puregene protocol (QIAGEN), whole-genome amplification (WGA) was performed in duplicate from both the HRS and the reactive cell sample as described previously (15).

Targeted Sequencing of Patient Samples

All DNA samples from the six newly processed cases were subjected to molecularly barcoded targeted sequencing of 43 genes recurrently mutated in myeloid neoplasms (QIAseq Targeted DNA Custom Panel–CDHS-13640Z-1040-Qiagen; Supplementary Table S1A), using 40 to 80 ng of input DNA. In addition, the microdissected HRS and reactive cell WGA DNA (250 ng) of case 1 was subjected to molecularly barcoded targeted sequencing of six JAK–STAT pathway genes recurrently mutated in cHL (QIAseq Targeted DNA Custom Panel–CDHS-16895Z-163-Qiagen; Supplementary Table S1B). Libraries were generated according to the manufacturer's instructions and sequenced on an Illumina MiSeq instrument for 2 × 151 cycles, using MiSeq Reagent Kit v2 or v3. The mean unique depth of coverage was 2,856× for the myeloid gene panel and 1,716× for the JAK–STAT pathway gene panel.

Bioinformatics Analysis of Targeted Sequencing Data

Bioinformatics mapping and variant calling of targeted sequencing data [European Nucleotide Archive (ENA) accession number PRJEB42867] was performed with QIAGEN smCounter algorithm v1 or v2 with default settings (27), and variant annotation was performed with Illlumina Variant Studio 3.0. Sequencing variants were then subjected to the further following filters and retained only if: (i) variants were predicted to change the gene coding sequence or involved the conserved splice-site (i.e., the four nucleotides surrounding the exon–intron junction); (ii) variants were not present in the Exome Aggregation Consortium (ExAC) database of normal individuals with a population frequency ≥1% (as provided by Illumina Variant Studio 3.0); (iii) variants were present at an allele frequency >2%; and (iv) indels were not located in homopolymeric stretches of five nucleotides or longer. In addition, variants called in HRS and reactive lymphoid cell WGA DNA had to be called in both WGA replicates and their mean weighted VAF (reported in Table 1) had to be >2%. The *SOCS1* disruptive mutation P83AfsX25 (a frameshift deletion of 26 nucleotides) was called in only one of the WGA HRS cell duplicates (VAF 98.6%; 72 unique supporting reads) due to poor coverage of this guanine-cytosine–rich gene in the other duplicate; in the latter, however, visual inspection of the BAM file showed

21/25 mutant raw reads, and the deletion was confirmed by standard Sanger sequencing of the same WGA DNA (cycling conditions and primers available upon request).

WES Analysis of Clonal Hematopoiesis in a Previous cHL Patient Cohort

We also analyzed our WES data from non-HRS cells of 34 cHL cases that we previously used as a matched counterpart to call somatic mutations in HRS cells of this malignancy (ref. 15; ENA accession number PRJEB25980). DNA from microdissected HRS and reactive cells had been subjected to duplicate WGA and independent WES of the duplicates (referred to as T1-T2 and N1-N2, respectively); furthermore, in most cases (26/34) unamplified genomic DNA from whole-blood leukocytes was also subjected to WES (15). Mean unique coverage was 157× for the 26 blood leukocyte samples and 149× for the 8 microdissected reactive sample pairs. Bioinformatics analysis focused on a target region of interest represented by 35 genes associated with age-related clonal hematopoiesis as defined by Tuval and Shlush (ref. 9 and Table 1 therein), whose genomic coordinates were retrieved from the NCBI Reference Sequence Database on human genome GRCh37.

Bioinformatics Reanalysis of WES Data

For each sample subjected to WES, the .mpileup file was generated by means of the SAMtools v.1.4 command mpilup with default parameters except disabling the base alignment quality computation [as recommended (28) for the subsequent Varscan2 variant calling; see further below] and increasing the minimum mapping quality from 0 to 1 while allowing a maximum depth of 1 billion (instead of 8,000) reads. We then called single-nucleotide variants and indels separately for each sample through Varscan2 (version 2.4.3) command mpileup2snp and mpileup2indel, respectively, using default settings (except that the minimum coverage depth to make a call was increased from 8 to 10, and the *P*-value threshold was changed from 0.99 to 0.05). Variant metrics were obtained by the bam-read count utility of Varscan2 with default parameters (except raising the minimum base quality from 0 to 20 in all supporting reads). Variants had then to pass Varscan2 fpfilter with default setting (except the minimum number of variant-supporting reads was changed from 4 to 2, and the minimum variant allele frequency was changed from 5% to 1%); we also retained variants with supporting reads that were nevertheless flagged as "NoReadCounts" by the fpfilter (this is a known bug of Varscan2). Moreover, regarding WGA samples, variants had to be called in both duplicates to efficiently control for false positives potentially introduced by the WGA step as described previously (15). Annotation of the variants was performed by both SNPEff (version n. 41/c) and wAnnovar (29), referring to the following database versions: 1000G: 2015 aug; ExAC: exac03; dbSNP: avsnp147; cosmic: cosmic81; clinvar: 20170501; and gnomAD: gnomAD_exome and gnomAD_genome (v.2). We then excluded variants with a gnomAD_genome frequency in normal individuals higher than 40%, and focused on sequence variants in coding exons or conserved splice sites. These variants were finally subjected to the further following filters and retained only if: (i) indels were not located in homopolymeric stretches of five nucleotides or longer; (ii) variants were present at an allele frequency of at least 2%; (iii) variants fulfilled the definition of a likely driver event according to functional experimental evidence (for the *CBL*^{G375S} variant, ref. 19, in case 2) or according to Abelson and colleagues (7); and (iv) variants were validated by molecularly barcoded targeted sequencing at high depth (mean unique coverage of 4,175×) following the same experimental and bioinformatics pipeline described in a previous section ("Bioinformatics analysis of targeted sequencing data") except that for case 2, validation was performed on whole-section DNA and that for the microdissected HRS and reactive cell samples of cases 4 and 5, we pooled the WGA DNA of the two replicates before library generation.

Authors' Disclosures

M.P. Martelli reports personal fees from AbbVie, Amgen, Pfizer, Jazz Pharmaceuticals, Novartis, and Janssen outside the submitted work. No disclosures were reported by the other authors.

Authors' Contributions

A. Venanzi: Conceptualization, data curation, formal analysis, methodology, writing–original draft, writing–review and editing. **A. Marra:** Conceptualization, data curation, formal analysis, methodology, writing–original draft, writing–review and editing. **G. Schiavoni:** Data curation, formal analysis, funding acquisition, methodology. **S.G. Milner:** Methodology. **R. Limongello:** Resources. **A. Santi:** Methodology. **V. Pettirossi:** Methodology. **S. Ultimo:** Methodology. **L. Tasselli:** Methodology. **A. Pucciarini:** Methodology. **L. Falini:** Resources. **S. Sciabolacci:** Resources. **M.P. Martelli:** Resources. **P. Sportoletti:** Methodology. **S. Ascani:** Histopathologic examinations of patients' specimens. **B. Falini:** Funding acquisition, writing–review and editing. **E. Tiacci:** Study direction, conceptualization, data curation, formal analysis, supervision, funding acquisition, writing–original draft, writing–review and editing.

Acknowledgments

This work was supported by a grant on cHL to E. Tiacci from AIRC (IG 2019, ID. 23732), a grant on AML to B. Falini from AIRC (IG 2019 number 23604), a grant on AML to B. Falini from ERC (Advanced Grant 2016 number 740230), the Leopold Griffuel prize from ARC to B. Falini, and a grant on cHL to G. Schiavoni from the Department of Medicine, University of Perugia (Ricerca di Base 2017–2019).

Received November 10, 2020; revised January 14, 2021; accepted March 2, 2021; published first April 10, 2021.

REFERENCES

1. Challen GA, Goodell MA. Clonal hematopoiesis: mechanisms driving dominance of stem cell clones. Blood 2020;136:1590–8.
2. Steensma DP, Bejar R, Jaiswal S, Coleman Lindsley R, Sekeres MA, Hasserjian RP, et al. Clonal hematopoiesis of indeterminate potential and its distinction from myelodysplastic syndromes. Blood 2015;126:9–16.
3. Jaiswal S, Fontanillas P, Flannick J, Manning A, Grauman PV, Mar BG, et al. Age-related clonal hematopoiesis associated with adverse outcomes. N Engl J Med 2014;371:2488–98.
4. Genovese G, Kahler AK, Handsaker RE, Lindberg J, Rose SA, Bakhoum SF, et al. Clonal hematopoiesis and blood-cancer risk inferred from blood DNA sequence. N Engl J Med 2014;371:2477–87.
5. Warren JT, Link DC. Clonal hematopoiesis and risk for hematologic malignancy. Blood 2020;136:1599–605.
6. Xie Mi, Lu C, Wang J, McLellan MD, Johnson KJ, Wendl MC, et al. Age-related mutation associated with clonal hematopoietic expansion and malignancies. Nat Med 2014;20:1472–8.
7. Abelson S, Collord G, Ng SWK, Weissbrod O, Mendelson Cohen N, Niemeyer E, et al. Prediction of acute myeloid leukemia risk in healthy individuals. Nature 2018;559:400–4.
8. Desai P, Mencia-Trinchant N, Savenkov O, Simon MS, Cheang G, Lee S, et al. Somatic mutations precede acute myeloid leukemia years before diagnosis. Nat Med 2018;24:1015–23.
9. Tuval A, Shlush LI. Evolutionary trajectory of leukemic clones and its clinical implications. Haematologica 2019;104:872–80.
10. Quivoron C, Couronné L, Della Valle V, Lopez CK, Plo I, Wagner-Ballon O, et al. TET2 inactivation results in pleiotropic hematopoietic abnormalities in mouse and is a recurrent event during human lymphomagenesis. Cancer Cell 2011;20:25–38.
11. Tiacci E, Venanzi A, Ascani S, Marra A, Cardinali V, Martino G, et al. High-risk clonal hematopoiesis as the origin of AITL and NPM1-mutated AML. N Engl J Med 2018;379:981–4.

12. Mathas S, Hartmann S, Küppers R. Hodgkin lymphoma: pathology and biology. Semin Hematol 2016;53:139–47.
13. Liu Y, Sattarzadeh A, Depstra A, Visser L, Van den Berg A. The microenvironment in classical Hodgkin lymphoma: an actively shaped and essential tumor component. Semin Cancer Biol 2014;24:15–22.
14. Reichel J, Chadburn A, Rubinstein P, Giulino-Roth L, Tam W, Liu Y, et al. Flow sorting and exome sequencing reveal the oncogenome of primary Hodgkin and Reed-Sternberg cells. Blood 2015;125:1061–72.
15. Tiacci E, Ladewig E, Schiavoni G, Penson A, Fortini E, Pettirossi V, et al. Pervasive mutations of JAK-STAT pathway genes in classical Hodgkin lymphoma. Blood 2018;131:2454–65.
16. Wienand K, Chapuy B, Stewart C, Dunford AJ, Wu D, Kim J, et al. Genomic analyses of flow-sorted Hodgkin Reed-Sternberg cells reveal complementary mechanisms of immune evasion. Blood Adv 2019;3:4065–80.
17. Schiavoni G, Tiacci E. Genetics of classical Hodgkin lymphoma. HemaSphere 2018;2:64–7.
18. Husby S, Favero F, Nielsen C, Sørensen BS, Bæch J, Grell K, et al. Clinical impact of clonal hematopoiesis in patients with lymphoma undergoing ASCT: a national population-based cohort study. Leukemia 2020;34:3256–68.
19. Reindl C, Quentmeier H, Petropoulos K, Greif PA, Benthaus T, Argiropoulos B, et al. CBL exon 8/9 mutants activate the FLT3 pathway and cluster in core binding factor/11q deletion acute myeloid leukemia/myelodysplastic syndrome subtypes. Clin Cancer Res 2009;15:2238–47.
20. Falini B, Mecucci C, Tiacci E, Alcalay M, Rosati R, Pasqualucci L, et al. Cytoplasmic nucleophosmin in acute myelogenous leukemia with a normal karyotype. N Engl J Med 2005;352:254–66.
21. Schmitz R, Wright GW, Huang DW, Johnson CA, Phelan JD, Wang JQ, et al. Genetics and pathogenesis of diffuse large B-cell lymphoma. N Engl J Med 2018;378:1396–407.
22. Reddy A, Zhang J, Davis NS, Moffitt AB, Love CL, Waldrop A, et al. Genetic and functional drivers of diffuse large B-cell lymphoma. Cell 2017;171:481–94.
23. Dominguez PM, Ghamlouch H, Rosikiewicz W, Kumar P, Béguelin W, Fontán L, et al. TET2 deficiency causes germinal center hyperplasia, impairs plasma cell differentiation, and promotes B-cell lymphomagenesis. Cancer Discov 2018;8:1632–53.
24. Kataoka K, Miyoishi H, Sakata S, Dobashi A, Couronné L, Kogure Y, et al. Frequent structural variations involving programmed death ligands in Epstein-Barr virus-associated lymphomas. Leukemia 2019; 33:1687–99.
25. Buscarlet M, Provost S, Zada YF, Bourgoin V, Mollica L, Dubé MP, et al. Lineage restriction analyses in CHIP indicate myeloid bias for TET2 and multipotent stem cell origin of DNMT3A. Blood 2018;132:277–80.
26. Young AL, Spencer Tong R, Birmann BM, Druley TE. Clonal hematopoiesis and risk of acute myeloid leukemia. Haematologica 2019; 104:2410–7.
27. Xu C, Nezami Ranjbar MR, Wu Z, Di Carlo J, Wang Y. Detecting very low allele fraction variants using targeted DNA sequencing and a novel molecular barcode-aware variant caller. BMC Genomics 2017;18:5.
28. Koboldt DC, Larson DE, Wilson RK. Using VarScan 2 for germline variant calling and somatic mutation detection. Curr Protoc Bioinformatics 2013;44:15.4.1–17.
29. Chang X, Wang K. wANNOVAR: annotating genetic variants for personal genomes via the web. J Med Genet 2012;49:433–6.